Viscoelasticity of aqueous telechelic poly(ethylene oxide) solutions: Relaxation and structure

L. A. Hough* and H. D. Ou-Yang
Department of Physics, Lehigh University, Bethlehem, Pennsylvania, 18015, USA
(Received 8 June 2005; published 3 March 2006)

We present a rheology study of associating polymers. The associating polymers are telechelic, composed of a water-soluble backbone (polyethylene oxide) terminated by hydrophobic moieties ($C_{16}H_{33}$). In aqueous solutions, these polymers self-assemble to form micellar structures. Above a critical concentration, approximately 1 wt % of polymer, bridging between the micelles forms a transient network. Traditionally, the viscoelastic response of these polymeric solutions has been described using the Maxwell model. In this work we measure the viscoelastic properties over an extended frequency range (0.01–6000 Hz) using microrheology, and show that at high frequencies the rheology behaves as the square root of the oscillation frequency. To fit the data, we use a combination of the Maxwell model and the Rouse model. The Maxwell model accounts for the hydrophobic associations between the polymeric micelles, and the Rouse model accounts for the microscopic dynamics of the individual micelles.

DOI: 10.1103/PhysRevE.73.031802 PACS number(s): 83.80.Rs, 87.80.Cc, 82.70.Dd, 83.80.Hj

I. INTRODUCTION

Telechelic polymers are often used as a model system for fundamental studies of associating polymers because they are architecturally simple. Telechelic polyethylene oxide (T-PEO) is composed of a long, water-soluble ethylene oxide midblock (M_n=10 000–100 000 g/mol) with each end terminated by hydrophobic alkane chains. In dilute, aqueous solutions, these polymers form micelles above a low critical micelle concentration ($<<$0.1 wt %) [1–3]. The core of a micelle is composed of the hydrophobic moieties and the corona is composed of loops formed by the midblocks [4]. As the polymer concentration is increased, the difunctional chains form bridges between the micelles, causing an effective attraction [3,5]. Increasing the concentration beyond the onset of bridging creates aggregates of micelles that percolate the sample volume and form a transient network [6]. The formation of a transient network is characterized by a strong increase in both the zero-shear viscosity and the complex shear modulus of the solution over a moderate increase in polymer concentration [6,7]. With a few exceptions [8,9], the frequency-dependent linear viscoelastic properties are described by a model that contains a single relaxation time and a plateau modulus, specifically, the Maxwell model [6,7,10].

Recently, fully end-capped telechelic polymers with a narrow molecular weight distribution have been shown to phase separate into a dense phase at the bottom of the sample and a dilute phase at the top of the sample [4,5]. This "gas-liquid" phase separation stems from the repulsion of the micelles due to the excluded volume and the attraction of the micelles due to bridging [4,5], and can be described by the adhesive sphere model [11]. The viscoelasticity, however, has traditionally been explained in terms of a transient network theory that effectively ignores the micellar nature of the solution, and predicts a Maxwellian behavior for the complex shear modulus [6,12]. When the micellar nature of the solution is taken into account, we expect that the complex shear modulus will deviate from the Maxwell model at time scales faster than the characteristic diffusion time of a single micelle.

In this paper, we determine the complex shear modulus of telechelic polymer solutions over a large dynamic range (0.01–6000 Hz) and concentration range (0.0125–4 wt %) using optical tweezers. Below a characteristic concentration of 1 wt %, the solutions are primarily viscous over the entire frequency range. Above 1 wt % we see the appearance of the viscoelastic behavior with a long relaxation time ($\sim$0.01 s) and an order of magnitude increase in the zero-shear viscosity. We interpret the appearance of a "slow" relaxation time and the increase in viscosity as a percolation transition. Above the percolation threshold, the viscoelastic properties are well described by the Maxwell model at low frequencies ($\omega<100$ rad/s). At large oscillation frequencies ($\omega>100$ rad/s), the real and imaginary parts of the complex shear modulus scale as the square root of the oscillation frequency. This scaling behavior prompts us to use the Rouse model to describe the relaxation mechanism at high frequencies. From the Rouse model, we determine a "fast" relaxation time that compares well to the characteristic diffusion time for an individual micelle [13,14]. The appearance of the fast and slow relaxation times has been confirmed by light scattering studies for a similar system [15]. Our study suggests that the micellar nature effects the viscoelastic properties at high frequencies, and that the transient network theory alone is not sufficient to account for the viscoelastic properties over a large dynamic range. In addition, the high-frequency behavior agrees with adhesive hard sphere theory in that the complex shear modulus scales as the square root of the oscillation frequency at high frequencies.

II. THEORY

A. Viscoelasticity of a transient network

Traditionally, the rheological properties of telechelic polymer solutions have been described in terms of the transient

*Present address: Rhodia, INC., 350 George Patterson Blvd., Bristol, PA 19007. Email address: larry.hough@us.rhodia.com

network theory [16]. This theory describes the real G' and imaginary G'' parts of the complex viscoelastic shear modulus in terms of the Maxwell model:

$$G'(\omega) = G_\infty \frac{\tau_M^2 \omega^2}{1 + \tau_M^2 \omega^2}, \tag{1}$$

$$G''(\omega) = G_\infty \frac{\tau_M \omega}{1 + \tau_M^2 \omega^2}, \tag{2}$$

where ω is the oscillation frequency. The plateau modulus is given by $G_\infty = \mu k_B T$, where μ is the number of elastically active chains in the network per unit volume, k_B the Boltzmann constant, and T the absolute temperature. The transient network theory was first proposed by Green and Tobolsky assuming rubber elasticity, but was extended by Tanaka and Edwards to include physical associations between polymers [12,16]. The characteristic time scale for the associations between the polymers is τ_M, the relaxation time of the system. Indeed, the relaxation time τ_M has been shown to increase exponentially with the size of the hydrophobic end cap, and it follows $\tau_M = \tau_0 e^{E/k_B T}$ (where E is the energy associated with the amount of attraction between the end cap and the micelle core) [6]. This relaxation time has been interpreted as the lifetime of a hydrophobe in a micelle, and the attempt time τ_0 has been shown to be proportional to the diffusion time of a single hydrophobe [7]. The transient network theory adequately describes the relaxation mechanisms and the origin of elasticity for telechelic polymer solutions. However, some studies have reported a slight deviation of the experimental data from Maxwellian behavior [8,9,17]; we believe this is because the transient network theory neglects the micellar nature of the material.

B. Viscoelasticity of adhesive spheres (i.e., sticky hard spheres)

Because Baxter's model has been used to describe the phase separation of telechelic polymer solutions, it is useful to derive the expected viscoelasticity for adhesive hard spheres to see if the model also describes the mechanical behavior of such systems. We use the formalism put forth by Cohen and co-workers who determined the viscoelasticity of a hard sphere system by expressing the frequency-dependent viscosity in terms of the equilibrium structure factor [13]. Here, we use the same concept to derive the viscoelasticity of adhesive spheres [14] (see the Appendix for details). The result for the complex shear modulus is

$$G(\phi,\omega) \approx \left(\frac{3k_B T\sqrt{\chi}\phi^2}{10\pi R^3}\right) \times \left[\frac{1+\phi/2}{(1-\phi)^2} - \lambda\phi\left(\frac{1}{1-\phi} + \frac{1}{12\phi} - \frac{\lambda}{12}\right)\right]^2 \sqrt{\tau_p \omega}(1+i). \tag{3}$$

Note, in Eq. (3), the contribution due to the viscosity of the background fluid, η_0, is excluded. Here, χ is the value of the pair correlation function at contact, and λ is related to the depth of the attractive potential energy between the particles (see the Appendix). Also, ϕ is the volume fraction of the adhesive spheres, and R is the radius of the spheres. The characteristic diffusion time for a single sphere $\tau_p = 6\pi\eta_0 R^3/k_B T$ is also referred to as the Péclet time [13]. In the limit of no attraction between the spheres, i.e., $\lambda = 0$, this expression reduces to the expression for hard spheres [with $\chi_{HS} = (1/2+\phi)/(1-\phi)$ [13]]. We would expect the real and imaginary parts of the complex viscoelastic modulus to vary as $\sqrt{\omega}$ at large oscillation frequencies for telechelic polymer solutions because the adhesive sphere theory describes the phase separation. Experimentally, this $\sqrt{\omega}$ behavior has been found to be true in hard sphere colloidal systems, as well as adhesive silica spheres [18,19].

C. Viscoelasticity of polymer chains composed of connected spheres

Because the viscoelasticity of adhesive spheres behaves like $\sqrt{\omega}$ at large frequencies, it may be interesting to examine if it is possible to describe data obtained from associating telechelic micelles in terms of the Rouse model. The Rouse model is defined as

$$G'(\omega) = G_\infty \sum_{p=1}^{N} \frac{\tau^2 \omega^2}{1 + \tau^2 \omega^2}, \tag{4}$$

$$G''(\omega) = G_\infty \sum_{p=1}^{N} \frac{\tau \omega}{1 + \tau^2 \omega^2}, \tag{5}$$

where $\tau = \tau_f / p^2$. In traditional polymer theory the longest relaxation time in the Rouse model is given by $\tau_f = \eta_B N^2 l_p^3 / \pi k_B T$ where l_p is the persistence length, N is the length of the polymer in units of persistence length, and η_B is the background viscosity [20]. The Rouse time τ_f is the time it takes the smallest segment to diffuse the persistence length. Rouse dynamics are derived from a microscopic model that assumes that the smallest segments of polymer are connected by springs. In other words, the Rouse model describes the dynamics of spherical monomers connected by springs. Therefore, it is reasonable to use this model to describe spherical micelles connected by associating bridges. The main distinction between the Rouse theory and the theory of adhesive spheres is the relaxation time τ_f. For adhesive spheres, we expect the Rouse time to be replaced by the Péclet time of the individual micelles. Therefore, in this study, we use the Rouse model to find a fast relaxation time and compare the relaxation time to the theoretically computed Péclet time for an individual micelle. Our interpretation of the fast relaxation time is in contrast with previous studies. Deviations from the Maxwell model have been measured previously in telechelic systems [21], and the two-step relaxation has been explained in terms of a slow relaxation due to the breakup of clusters, and a fast relaxation due to the lifetime of the hydrophobes in the micelle.

D. Derivation of the Péclet time for spherical micelles

To theoretically determine the Péclet time, the Daoud-Cotton model is used to determine the thermodynamic radius of the micelles [4,22]. The model views a micelle as a series of radially growing space-filling blobs and is related to the

TABLE I. Molecular weight and Péclet time.

M_n(kg/mol)	$2N_s$	R (nm)	Péclet time (μs)
100.4	1042	29.3	120.0
84.3	875	25.6	79.0
67.6	709	23.1	57.0
51	531	19.5	35.0

number of arms in the micelle, $2p$. Because the arms are composed of loops, we ignore the midpoint connection, effectively cutting the chain in half. In a good solvent, the root mean square end-to-end distance of a polymer chain depends on the excluded volume v/l_p^3, the number of segments per half chain, N_s, and the persistence length l_p, and is given by [4,20]

$$s = \left(\frac{v}{2l_p^3}\right)^{1/5} N_s^{3/5} l_p. \tag{6}$$

The micelle radius is then given by $R=1.172p^{1/5}s$ [4]. The persistence length is taken to be $l_p=0.44$ nm for polyethylene oxide; $v/l_p^3=0.3$ because water is a good solvent [4]. The aggregation number p has been measured for polymers similar to those used in this study by a variety of techniques. Fluorescent studies have shown that the aggregation number is 10 ± 1 for polymer molecular weights between 34 and 50 kg/mol [23], whereas dynamic light scattering, viscometry, and NMR studies have shown that the aggregation number is 23 ± 1 for a polymer molecular weight of 34 kg/mol [1,24,25]. The discrepancy in the aggregation number does not drastically affect the theoretically determined radius, because of the weak dependence of the radius on aggregation number. A value of either 10 ± 1 or 23 ± 1 for the aggregation number results in $\sim$10% discrepancy between the calculated radii. In this study, we use an aggregation number of 23 and we assume that the aggregation number is independent of molecular weight. In addition, we have assumed that the micelle size does not depend on concentration; this assumption is reasonable as long as the concentration is lower than that where the micelles start to overlap [3]. The theoretically determined radii are used to estimate the Péclet time for a spherical micelle. The number of subunits, N_s, is calculated by assuming two monomers per persistence length. Table I shows the calculated radii and the Péclet time for the various molecular weight polymers used in this study [26]. The Péclet time is calculated assuming $\eta_0=0.01$ P, the viscosity of water.

III. EXPERIMENT

A. Materials

Samples of polyethylene oxide end capped by $C_{16}H_{33}$ with number average molecular weight of $M_n=51$, 67.6, 84.3, 100.4 kg/mol were provided by Union Carbide. The polydispersity of the telechelic samples M_w/M_n is 1.7 as determined by gel permeation chromatography [27]. The polymers have incomplete end capping, reported to be 1.4–1.7 hydrophobes per chain for polymers of molecular weight $M_n=34$ and 51 kg/mol, respectively [28]. Because of the incomplete end capping, phase separation is not observed in our samples [4,6]. Solutions were prepared by mixing the $M_n=67.6$ kg/mol polymer with filtered (0.2 μm Nalgene) deionized water, to concentrations of 0.125, 0.25, 0.5, 0.75, 1.0, 1.5, 2.5, and 4.0 wt %. Samples were seeded with a small amount of silica particles (volume fraction $\phi_P<10^{-5}$) of diameters 0.7, 1.6, and 2.9 μm for use as probes in the microrheology study. Samples of 1 wt % were used for all the other molecular weights.

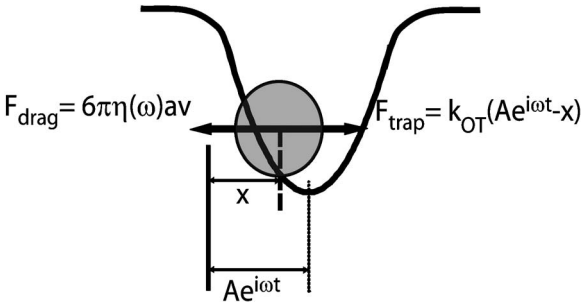

FIG. 1. Diagram of the forces on a colloidal particle in an oscillating optical trap embedded in a viscoelastic medium.

B. Bulk rheology techniques

Linear bulk viscoelasticity data were taken with a Rheometrics RDAII rheometer with a cone and plate geometry. The results were independent of the tool geometry. The viscoelasticity as a function of strain amplitude was also taken to ensure that the viscoelastic data were obtained in the linear regime. For solutions at concentrations $c<2.5$ wt %, bulk rheology measurements by the RDAII are not possible due to the low viscosity of the sample. All measurements were performed at room temperature $\sim$23 °C.

C. Microrheology technique

The complex shear modulus was determined by using an oscillating optical tweezers technique. The oscillating optical tweezers apparatus has been described in detail elsewhere [29,30]. Briefly, a colloidal probe particle is held by an optical trap. The optical trap is oscillated by a piezoelectric mirror at a set frequency ω and amplitude A. The force imparted on the particle by the optical trap can be approximated by Hooke's law, with an effective spring constant k_{ot}. The force due to the trap is the effective spring constant multiplied by the distance between the center of the particle and the center of the trap. The particle also experiences a drag force as it is oscillated through the fluid (see Fig. 1). For a simple viscous liquid, the drag force is taken to be $6\pi\eta av$, where η is the zero shear viscosity of the liquid, and v is the velocity of the particle. For a viscoelastic fluid we make the assumption that the viscosity is a frequency-dependent complex function. The complex viscosity is then related to the complex shear modulus by $G(\omega)=\eta(\omega)\omega$, and the equation of motion for the particle becomes

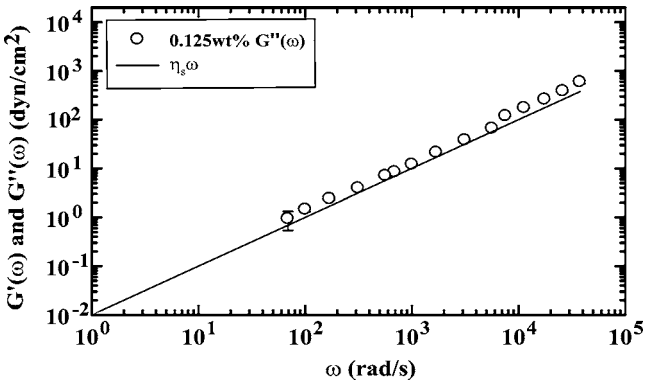

FIG. 2. The imaginary part of the complex shear modulus for a 0.125 wt % aqueous solution of M_n=67.6 kg/mol telechelic PEO probed by a 1.6 μm diameter silica probe particle with the oscillating optical tweezers technique. The solid line indicates the viscous contribution from the solvent, $G''=\eta_s\omega$, where η_s=0.01 P, the viscosity of water at room temperature.

$$m\ddot{x} = -6\pi a\eta(\omega)\dot{x} + k_{ot}(Ae^{i\omega t} - x). \tag{7}$$

The restoring force due to the optical trap is given by $k_{ot}(x-A)$ because $A-x$ is the colloidal particle's distance from the center of the optical trap. The motion of the particle, x, is $D(\omega)e^{i[\omega t-\delta(\omega)]}$, where $D(\omega)$ is the amplitude of particle's displacement, and $\delta(\omega)$ is the phase of the particle's motion. We neglect the inertia of the particle and the fluid, so the viscoelastic storage and loss modulus are given by

$$G'(\omega) = \frac{k_{ot}}{6\pi a}\left(\frac{A\cos\delta(\omega)}{D(\omega)} - 1\right), \tag{8}$$

$$G''(\omega) = \frac{k_{ot}}{6\pi a}\left(\frac{A\sin\delta(\omega)}{D(\omega)}\right). \tag{9}$$

Experimentally, the oscillatory motion of the particles is measured by detecting the light scattered from the optically trapped particle using a split photodiode and feeding the signal into a lock-in amplifier (see Ref. [30]). We use a lock-in amplifier because it allows us to measure both D and δ of the particle's motion as a function of ω. Because the lock-in amplifier retains the phase information (unlike studies of the thermal motions of tracer particles) the micromechanical properties of soft materials can be directly determined, provided that the effective spring constant of the optical trap is known. The effective spring constant is calibrated by measuring the magnitude and the phase of a particle's displacement in a liquid of known viscosity (water). In all the experiments done in this study, the oscillation frequency of the piezoelectric mirror was varied discretely from 0.1 to 6000 Hz, and the oscillation amplitude was kept at $A\sim 40$ nm.

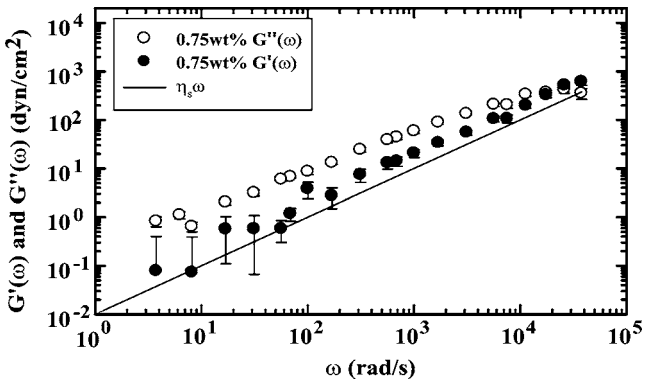

FIG. 3. The real and imaginary parts of the complex shear modulus for a 0.75 wt % aqueous solution of M_n=67.6 kg/mol telechelic PEO probed by a 1.6 μm diameter silica probe particle with the oscillating optical tweezers technique. The solid line indicates the viscous contribution from the solvent, $G''=\eta_s\omega$, where η_s=0.01 P, the viscosity of water at room temperature.

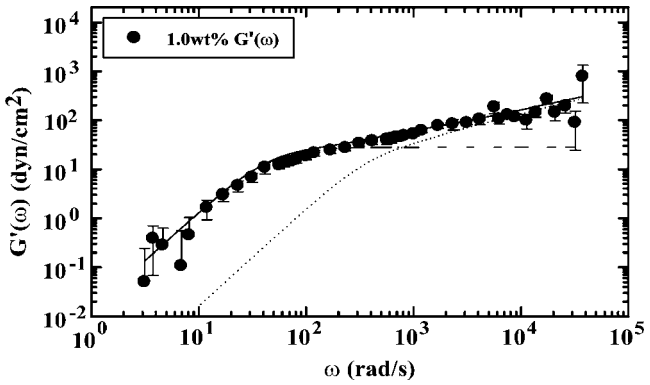

FIG. 4. The real part of the complex shear modulus for a 1.0 wt % aqueous solution of M_n=67.6 kg/mol telechelic PEO probed by a 1.6 μm diameter silica probe particle.

IV. RESULTS AND DISCUSSION

Measurements of the complex shear modulus for 0.125 wt % aqueous solutions of 67.6 kg/mol telechelic PEO probed by a 1.6 μm diameter silica probe particle with the oscillating optical tweezers technique are shown in Fig. 2. For this concentration, the viscoelastic storage modulus G' was not measurable. These results indicate that the solutions are more liquid than solid for the entire frequency range. Because the loss modulus is nearly linear as a function of

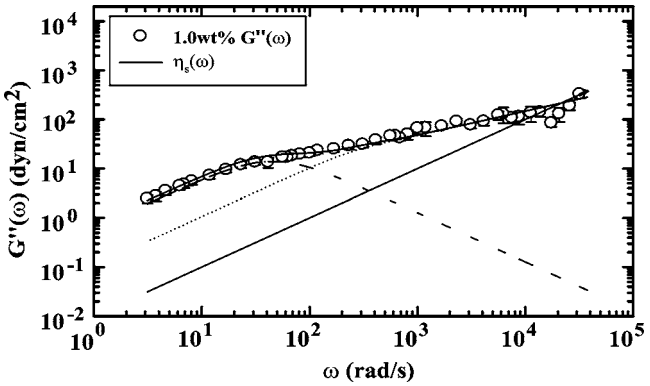

FIG. 5. The imaginary part of the complex shear modulus corresponding to Fig. 4. The solid line indicates the viscous contribution from the water.

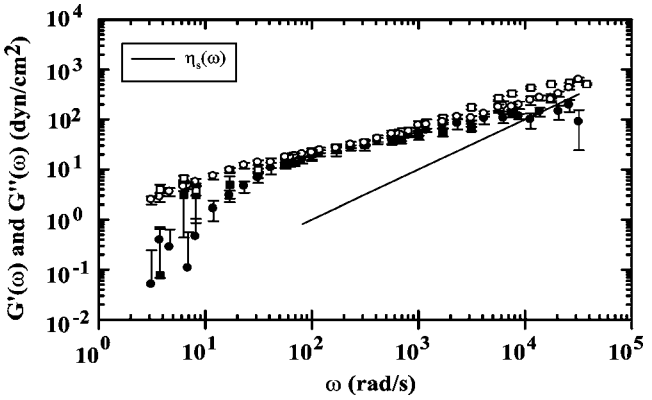

FIG. 6. The real (closed symbols) and imaginary (open symbols) parts of the complex shear modulus for a 1.0 wt % aqueous solution of M_n=67.6 kg/mol telechelic PEO probed by a 1.6 (circles) or a 0.7 (squares) μm diameter silica probe particle with the oscillating optical tweezers technique.

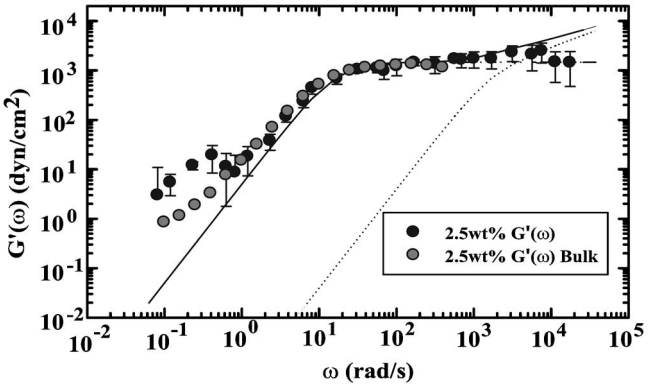

FIG. 7. The real part of the complex shear modulus for a 2.5 wt % aqueous solution of M_n=67.6 kg/mol telechelic PEO probed by a 1.6 μm diameter silica probe particle. The dark gray symbols represent the imaginary part of the complex shear modulus as measured by a bulk rheology technique.

frequency, the zero-shear viscosity of these samples could be determined by extrapolating the loss modulus to zero frequency (specifically lim $\omega \to 0$, $\eta_0 = G''/\omega$). The solid line indicates the viscous contribution from the solvent, η_s =0.01 P, the viscosity of water at room temperature. The results are similar for 0.25 and 0.5 wt % (data not shown), but showed an increase in the measured viscosity.

A measurable G' begins to appear at a concentration of 0.75 wt % for aqueous solutions of 67.6 kg/mol T-PEO, shown in Fig. 3. Although we do not see the appearance of an extended plateau modulus, we do see the intersection of G' and G'' indicating that there is a fast relaxation time at high frequencies. We attribute the fast relaxation time to the dynamics of individual micelles. The absence of either a slow relaxation time or a plateau modulus simply means that this concentration is slightly below what is needed to form bridges between the micelles.

Figures 4 and 5 show the real and imaginary components of the viscoelastic shear modulus, for a 1 wt % solution (M_n=67.6 kg/mol). For this solution, we see the appearance of a slow relaxation time at 0.022 s but the response is not purely Maxwellian, as is expected for telechelic polymer solutions [6,7]. Indeed, the low-frequency data can be described with the Maxwell model, and the dashed line indicates a fit to Eq. (1) at low frequencies using two fitting parameters G_∞ and τ_M. The zero-shear viscosity is given by $G_\infty \tau_M$. Although the Maxwell model fits these data well at low frequencies, the deviation is significant at large frequencies. To this end, we use the Rouse model to describe the data at larger frequencies. Please note that the Rouse model is a sum of Maxwell functions, and is identical to the Maxwell model at time scales larger than τ_f. At time scales smaller than τ_f the plateau disappears because it is smeared out by many fast relaxation processes. The dotted lined indicates a fit to Eq. (4), using a single fitting parameter τ_f. The plateau modulus G_∞ used in the Rouse model is *identical* to the plateau modulus found from fitting the Maxwell model to the low-frequency data. The solid line through the data is the sum of the contributions from the Maxwell model and the Rouse model. Similar behavior is seen for other molecular weights, and although the frequency-dependent data are not presented here, the results for each τ_f are shown in Table II.

Because the Maxwell model combined with the Rouse model is used to determine relaxation times that are related to the microscopic structure, it is important to confirm that the viscoelastic properties are independent of the probe particle size. Recently it has been shown that the microrheology is sensitive to particle size for samples that are inhomogeneous on the length scale of the particle [31]. Therefore, measurements of different particle sizes are taken to see if the microrheological properties are affected by inhomogeneity in the sample. In Fig. 6 we show that the measured rheological properties determined by the oscillating optical tweezers technique are not sensitive to particle size.

At 2.5 wt % the viscoelasticity of the 67.6 kg/mol T-PEO solutions is large enough to measure with a conventional rheometer. Figures 7 and 8 show the real and imaginary components of the viscoelastic shear modulus. As before, the line through the data is a summation of the fits to the Maxwell

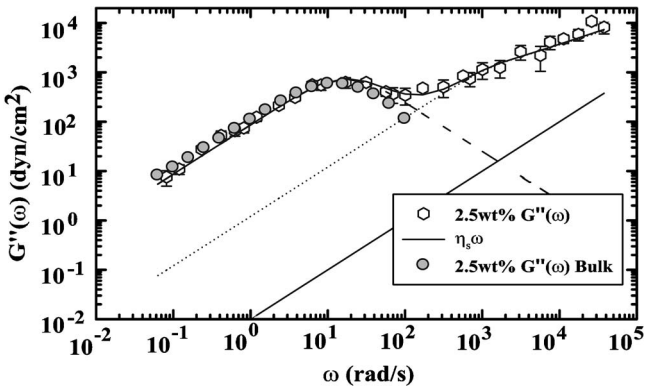

FIG. 8. The real part of the complex shear modulus for a 2.5 wt % aqueous solution of M_n=67.6 kg/mol telechelic PEO probed by a 1.6 μm diameter silica probe particle. The dark gray symbols represent the imaginary part of the complex shear modulus as measured by a bulk rheology technique. The solid line indicates the viscous contribution from the solvent, $G'' = \eta_s \omega$, where η_s=0.01 P, the viscosity of water at room temperature.

TABLE II. A comparison between the fast relaxation time obtained by the Rouse model and the calculated Péclet time.

M_w(kg/mol)	c (wt %)	$\tau_f(\mu s)$	$\tau_{calc}(\mu s)$
67.6	0.75	44.0	57.0
67.6	1.0	2.3×10^3	3.7×10^3
67.6	1.5	1.8×10^3	240.0
67.6	2.5	50.0	57.0
67.6	4.0	26.0	57.0
100.4	1.0	640.0	120.0
84.3	1.0	1.6×10^3	1.3×10^4
51.0	1.0	650.0	660.0

and Rouse models. The dark gray symbols represent the components of the complex shear modulus as measured by bulk rheology and compare well to the microrheology. The bulk rheological behavior appears to be nearly Maxwellian at the frequencies accessible to the rheometer. It is therefore not surprising that a network of associating micelles was traditionally described in terms of the transient network theory (Maxwell model). Only by assessing higher frequencies can the deviations in the viscoelasticity from Maxwellian behavior due to the micellar nature of the medium be observed. As a confidence check, data were taken with 0.7 and 2.9 μm probe particles; every probe particle size tested gave the same results within the error of the measurements (data not shown).

As shown in Fig. 9 the fast relaxation times found from the Rouse model compare well to the Péclet time for an individual micelle ($\sim$60.0 μs for M_n=67.6 kg/mol). Interestingly, however, the fast relaxation times are dependent on polymer concentration. This dependence can be attributed to the behavior of the micellar network, as indicated by the plateau modulus. Figure 10 shows the plateau modulus, as a function of concentration, found by fitting the Maxwell model to the low-frequency data. At 1 wt % the plateau modulus is 28 dyn/cm^2. If every micelle constituted a link in the elastically active network, the plateau modulus would be given by $G_\infty = FnkT = 108$ dyn/cm^2 from the theory of rubber elasticity. Here n is the number of micelles per unit volume and F is the faction of fully end-capped polymers, approximately 0.7 for this system. The discrepancy between the measured plateau modulus and the expected plateau modulus implies that approximately four micelles are connected together to form an elastically active chain or "superbridge" [6]. These micelles would move as a unit, effectively increasing the radius used to theoretically determine the Péclet time. Table II shows the comparison between the Péclet time determined by rescaling the micellar radius and the fast relaxation time determined from fitting the Rouse model to the data for various polymer concentrations (M_n=67.6 kg/mol), as well as various polymer molecular weights. Although this explanation for the variation of τ_f with concentration is plausible, we should point out that the micellar radius could change with concentration, thus changing τ_f. Further studies are needed to fully justify this assumption.

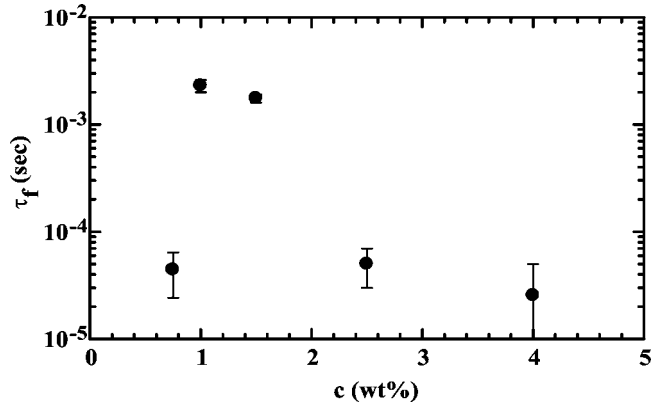

FIG. 9. The behavior of the fast relaxation time as determined from the Rouse model, for various concentrations of T-PEO (M_n =67.6 kg/mol).

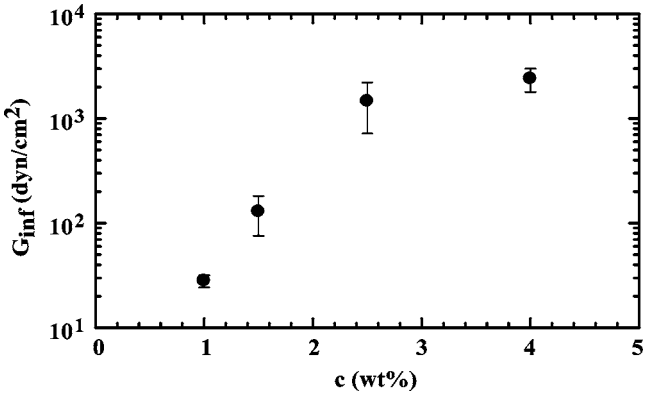

FIG. 10. The concentration dependence of the plateau modulus obtained by the Maxwell model for T-PEO (M_n=67.6 kg/mol).

Figure 11 shows the zero-shear viscosity as a function of concentration. The viscosity increases by more than an order of magnitude between 0.75 and 1 wt %. According to the adhesive hard sphere theory, the increase is most likely due to a percolation transition between these two concentrations. Here percolation refers to an infinite cluster (network) of micelles at very long time scales [32]. Percolation is typical for polymeric media and is characterized experimentally by a large increase in viscosity [33]. In addition, the solution must

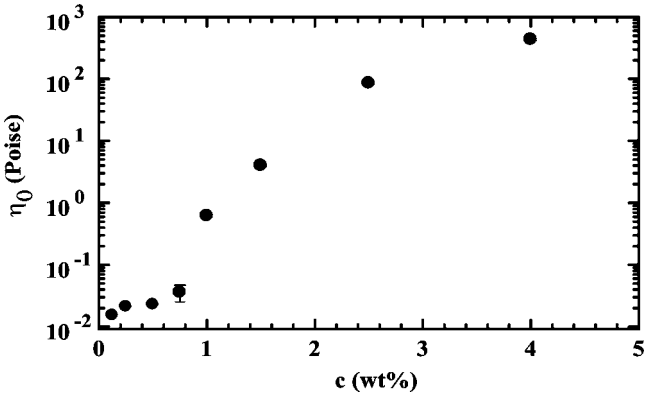

FIG. 11. The dependence of the zero-shear viscosity on the concentration for M_n=67.6 kg/mol TPEO.

exhibit a measurable transition from a simple liquid medium to an elastic medium [20]. Indeed, at 1 wt % there is an appearance of a long relaxation time and a plateau modulus. For similar polymer solutions, the percolation concentrations have been found to be 4.5, 2.7, 2.3, 2.1, 1.9, and 1.6 wt % for polymers that have a fraction of end capping equal to 0.2, 0.4, 0.5, 0.6, 0.75, and 1.0 [5]. The appearance of the increased viscoelasticity is independent of a glass transition [34]; at no point did we see a divergence in the viscosity or a kinetic arrest of the solution despite the fact that the micelles were sightly compressed. At micellar volume fractions much greater than 1 ($c>>2.5$ wt %), we would expect that the micelles would lose their individual identity, and the adhesive sphere model would no longer be applicable.

V. SUMMARY

The microrheology of concentrated telechelic polymer solutions is described by contributions from the Maxwell model and the Rouse model. The longer relaxation time is interpreted as the disengagement time of a hydrophobe from a micelle; the shorter relaxation time is on the order of the characteristic diffusion time for a single micelle. When we rescale the groups of micelles that behave like an elastically active chain as if they were a single micelle, we find that the measured fast relation times correspond well to the rescaled characteristic diffusion times. The high-frequency behavior of the shear modulus in the Rouse model is identical to the behavior predicted by adhesive hard sphere theory, namely, $\sqrt{\omega}$ at frequencies greater than the inverse of the fast relaxation time.

ACKNOWLEDGMENTS

The authors thank Dr. Richard Jenkins of Dow Chemical (formerly with Union Carbide) for providing the polymer samples used in this study. The project was funded in part by a grant from PA-DCED Center for Optical Technologies, Lehigh University.

APPENDIX

The interparticle potential for the adhesive hard sphere theory consists of a repulsive hard core potential, and an attractive square well potential

$$\frac{V(r)}{k_BT}=\begin{cases}\infty & \text{for } 0<r<2R',\\ \ln\left(12\xi\dfrac{R-R'}{R}\right) & \text{for } 2R'<r<2R,\\ 0 & \text{for } r>2R.\end{cases} \tag{A1}$$

Here R is the radius of the adhesive sphere, and $2R-2R'$ is the width of the attractive square well. In the limit of the "stickiness" parameter $1/\xi$ going to zero, this reduces to a hard sphere interaction potential.

The derivation of the complex shear modulus for adhesive hard spheres starts with the structure factor which has been derived elsewhere [11,14]. For simplicity, we only consider the limit where the width of square well vanishes [11],

$$\frac{1}{S(x)}-1=24\phi\left(\alpha f_2(x)+\beta f_3(x)+\frac{\alpha}{2}\phi f_5(x)\right)+2\phi^2\lambda^2 f_1(x)-2\phi\lambda f_4 \tag{A2}$$

where

$$\lambda=\frac{6(\Delta-\sqrt{\Delta^2-\Gamma})}{\phi},$$

$$\Delta=\xi+\phi/l,$$

$$l=1-\phi,$$

$$\Gamma=\frac{\phi(1+\phi/2)}{3l^2},$$

$$\alpha=\frac{(1+2\phi-\lambda\phi l)^2}{l^4},$$

$$\beta=\frac{-3\phi(2+\phi)^2+2\lambda\phi l(1+7\phi+\phi^2)-(\lambda\phi l^2(2+\phi)}{2l^4}. \tag{A3}$$

The functions $f_n(x)$ are given by

$$f_1(x)=\frac{1-\cos x}{x^2},$$

$$f_2(x)=\frac{\sin x-x\cos x}{x^3},$$

$$f_3(x)=\frac{2x\sin x-(x^2-2)\cos x-2}{x^4},$$

$$f_4(x)=\frac{\sin x}{x},$$

$$f_5(x)=\frac{(4x^3-24x)\sin x-(x^4-12x^2+24)\cos x+24}{x^6}. \tag{A4}$$

Here $x=2Rk$. The structure factor for adhesive spheres is a function of the volume fraction ϕ and the stickiness parameter $1/\xi$. Following the work of Cohen and co-workers for hard spheres, the high-frequency behavior of the viscosity

for adhesive spheres in the limit of large wave vector is given by [13,14]

$$\eta(\phi,\omega) = \frac{k_B T}{60\pi^2 \eta_0} \int dk\, k^4 \left(\frac{S'(k)}{S(k)}\right)^2 \frac{1}{2\omega_H(k) - i\omega} \quad \text{(A5)}$$

where $\omega_H(k) = D_0 k^2 / \chi S(k) d(k)$ is the linewidth of the dynamic structure factor $S(k,\omega)$, and $d(k) = 1 - j_0(2Rk) + 2j_2(2Rk)$ where $j_n(x)$ is the spherical Bessel function of the nth order. Here $D_0 = k_B T / 6\pi\eta_0 R$ and χ is the value of the pair correlation function at contact [14]. Taking the necessary integrals, in the limit of large k, the frequency-dependent viscosity is

$$\eta(\phi,\omega) \approx \eta_0 + \frac{9\eta_0}{5}\left\{\phi\left[\alpha\left(1+\frac{\phi}{2}\right)+\beta\right] - \frac{\phi\lambda}{12} + \frac{\phi^2\lambda^2}{12}\right\}^2 \times \sqrt{\frac{\chi}{\tau_p\omega}}(1+i). \quad \text{(A6)}$$

If we assume that $G(\omega) = \eta\omega$ and rearrange the constants, the complex shear modulus is given as

$$G(\phi,\omega) \approx \eta_0\omega + \frac{3k_B T\sqrt{\chi}\phi^2}{10\pi R^3}\left[\frac{1+\phi/2}{(1-\phi)^2} - \lambda\phi\left(\frac{1}{1-\phi} + \frac{1}{12\phi} - \frac{\lambda}{12}\right)\right]^2 \sqrt{\tau_p\omega}(1+i). \quad \text{(A7)}$$

[1] M. A. Winnik and A. Yetka, Curr. Opin. Colloid Interface Sci. **2**, 424 (1997).
[2] Y. Séréro, R. Aznar, G. Porte, J.-F. Berret, D. Calvet, A. Collet, and M. Viguier, Phys. Rev. Lett. **81**, 5584 (1998).
[3] A. N. Semenov, J-F. Joanny, and A. R. Khokhlov, Macromolecules **28**, 1066 (1995).
[4] Q. T. Pham, W. B. Russel, J. C. Thibeault, and W. Lau, Macromolecules **32**, 2996 (1999).
[5] F. Lafleche, D. Durand, and T. Nicolai, Macromolecules **36**, 1331 (2003).
[6] T. Annable, R. Buscall, R. Ettelaie, and D. Whittlestone, J. Rheol. **37**, 695 (1992).
[7] Q. T. Pham, W. B. Russel, J. C. Thibeault, and W. Lau, Macromolecules **32**, 5139 (1999).
[8] J. F. Le Meins and J. F. Tassin, Colloid Polym. Sci. **281** 283 (2003).
[9] W. K. Ng, K. C. Tam, and R. D. Jenkins, J. Rheol. **44**, 137 (2000).
[10] R. D. Jenkins, Ph.D. thesis, Lehigh University, Bethlehem, PA, 1990 (unpublished).
[11] R. J. Baxter, J. Chem. Phys. **48**, 2770 (1968).
[12] F. Tanaka and S. F. Edwards, J. Non-Newtonian Fluid Mech. **43**, 247 (1992).
[13] I. M. de Schepper, H. E. Smorenburg, and E. G. D. Cohen, Phys. Rev. Lett. **70**, 2178 (1993).
[14] Y. C. Liu, S. H. Chen, and J. S. Huang, Phys. Rev. E **54**, 1698 (1996).
[15] B. Nystrom, H. Walderhaug, and F. K. Hansenm, J. Chem. Phys. **97**, 7743 (1993).
[16] M. S. Green and A. V. Tobolsky, J. Chem. Phys. **14**, 80 (1946).
[17] N. Cathebras, A. Collet, M. Viguier, and J. F. Berret, Macromolecules **31**, 1305 (1998).
[18] T. G. Mason and D. A. Weitz, Phys. Rev. Lett. **75**, 2770 (1995).
[19] A. T. J. M. Woutersin, J. Mellema, C. Blom, and C. G. de Kruif, J. Chem. Phys. **101**, 542 (1994).
[20] M. Doi and S. F. Edwards, *The Theory of Polymer Dynamics* (Clarendon, Oxford, 1992).
[21] D. Bedrov, G. D. Smith, and J. F. Douglas, Europhys. Lett. **59**, 384 (2002).
[22] M. Daoud and J. P. Cotton, J. Phys. (Paris) **43**, 531 (1982).
[23] Y. Wang and M. A. Winnik, Langmuir **6**, 1437 (1990).
[24] P. M. Macdonald, Y. Uemura., L. Dyke, and X. Zhu, Adv. Chem. Ser. **248**, 337 (1996).
[25] T. Kato, K. Nakamur, M. Kawaguchi, and A. Takaha, Polym. J. (Tokyo, Jpn.) **13**, 1037 (1981).
[26] Rouse type dynamics would also exist for the individual chain segments of the polymer. However, the Rouse time for the polymer $\sim 10^{-6}$ s is approximately an order of magnitude faster than the Péclet time $\sim 10^{-5}$ s for every molecular weight. The individual chain dynamics would occur at frequencies larger than the adhesive sphere dynamics.
[27] A. Yekta, J. Duhamel, P. Brochard, H. Adiwidjaja, and M. A. Winnik, Macromolecules **26**, 1829 (1993).
[28] A. Yekta, B. Xu, J. Duhamel, H. Adiwidjaja, and M. A. Winnik, Macromolecules **28**, 956 (1995).
[29] H. D. Ou-Yang, in *Polymer-Colloid Interactions: From Fundamentals To Practice*, edited by P. Dubin, (John Wiley and Sons, New York, 1999), p. 385–405.
[30] L. A. Hough and H. D. Ou-Yang, Phys. Rev. E **65**, 021906 (2002).
[31] D. T. Chen, E. R. Weeks, J. C. Crocker, M. F. Islam, R. Verma, J. Gruber, A. J. Levine, T. C. Lubensky, and A. G. Yodh, Phys. Rev. Lett. **90**, 108301 (2003).
[32] M. E. Cates, T. C. B. McLeish, and M. Rubinstein, J. Phys.: Condens. Matter **2**, 749 (1990).
[33] L. Lobry, N. Micali, F. Mallamace, C. Liao, and S.-H. Chen, Phys. Rev. E **60**, 7076 (1999).
[34] E. Zaccarelli, G. Foffi, K. A. Dawson, F. Sciortino, and P. Tartaglia, Phys. Rev. E **63**, 031501 (2001).